

Woods Hole Oceanographic Institution



An All-Thermistor Pyrgeometer

by

Richard E. Payne

Woods Hole Oceanographic Institution

December 2004

Technical Report

Funding was provided by the National Science Foundation under Contract Number OCE98-18470.

Approved for public release; distribution unlimited.



Upper Ocean Processes Group
Woods Hole Oceanographic Institution
Woods Hole, MA 02543
UOP Technical Report 2004-02

WHOI-2004-07
UOP-2004-02

An All-Thermistor Pyrgeometer

by

Richard E. Payne

December 2004

Technical Report

Funding was provided by the National Science Foundation
under Contract Number OCE98-18470.

Reproduction in whole or in part is permitted for any purpose of the United States
Government. This report should be cited as Woods Hole Oceanog. Inst. Tech. Rept.,
WHOI-2004-07.

Approved for public release; distribution unlimited.

Approved for Distribution:



Nelson G. Hogg, Chair

Department of Physical Oceanography

Abstract

The design and testing of an all-thermistor (no thermopile) pyrometer (LWT) is described. After calibration by comparison with a Kipp & Zonen CG4, 9.2 months of data show mean differences of order $1-2 \text{ W m}^{-2}$ with standard deviations of order $7-8 \text{ W m}^{-2}$. Approximately half of the mean difference and the standard deviation derived from 40 occasions when the LWT readings were anomalously high for periods of 2-14 hours, principally at night. No reason has been found for the anomalous behavior. During the 9.2 months of data, there were also 11 periods of a few hours each when the Eppley PIR indicated noticeably higher flux values than did the Kipp & Zonen CG4.

The conclusion reached is that contemporary thermistors allow temperature measurements of sufficient accuracy, and the thermopile can be eliminated from pyrometers. The differences seen between the Kipp & Zonen and the Eppley raise doubts about their absolute accuracies on time scales of hours, although their long-term averages are quite comparable.

Table of Contents

Abstract.....	iii
List of Tables	v
List of Figures.....	vi
1. Introduction.....	1
2. PIR Operation	1
3. A New Pyrgeometer.....	3
4. Accuracy	4
5. Calibration.....	5
6. Data Set.....	5
7. Anomalous Data.....	6
8. Comparison.....	6
9. Conclusion	8
10. Acknowledgments.....	8
11. References.....	9

List of Tables

Table 1: Calibration Constants.....	5
Table 2: Pyrgeometer mean differences and standard deviations, 9.2 months of data.....	7
Table 3: Pyrgeometer mean differences and standard deviations, year day 280-299.....	7
Table 4: Overall longwave flux averages	8

List of Figures

Figure 1: L/R: The Eppley PIR, Kipp & Zonen CG4, and a thermistor pyrgeometer.....	11
Figure 2: Cross-section sketch of the all-thermistor pyrgeometer.....	12
Figure 3: Sketch of the Kipp & Zonen CG4 pyrgeometer. Labeled parts are: (A) desiccant; (B) white sun screen; (C) body temperature thermistor; (D) thermal detector; (E) silicon window; (F) sub frame.	13
Figure 4: Sketch of the Eppley PIR. (A) top and dome mount (stainless steel); (B) pyrgeometer body (cast bronze); (C) hole in which body thermistor is potted; (D) thermopile; (E) thermal detector; (F) internal radiation shield (aluminum); and (G) silicon window.....	13
Figure 5: Radiometer calibration facility on roof of Clark Laboratory, Woods Hole, MA. The Kipp & Zonen CG4, Eppley PIR, Eppley/IMET PSP and Eppley/IMET PIR are in the foreground. An LWT is at the top of each of the two long tubes just beyond.....	14
Figure 6: Example of elevated values of total longwave flux of LWT001, LWT002 and IMET PIR (dotted lines) relative to the Kipp & Zonen CG4 (solid line) and Eppley PIR (dashed line).....	15
Figure 7: Example of elevated values of total longwave flux of the LWT001, LWT002 and the IMET PIR (dotted lines) and the Eppley PIR (dashed line) relative to the Kipp & Zonen CG4 (solid line).....	16
Figure 8: Total longwave flux of thermistor pyrgeometer LWT001 vs. Eppley PIR.....	17
Figure 9: Total longwave flux of thermistor pyrgeometer LWT002 vs. Eppley PIR.....	18
Figure 10: Total longwave flux of Kipp & Zonen CG4 (solid line), Eppley PIR (dashed line), and LWT001, LWT002 (dotted lines), 7-26 October 2002.....	19
Figure 11: Difference between LWT001 (solid line), LWT002 (dotted line) and Kipp & Zonen CG4 total longwave fluxes, 7-26 October 2002.....	20
Figure 12: Difference between Eppley PIR and Kipp & Zonen CG4 total longwave fluxes, 7-26 October 2002.....	21
Figure 13: Shortwave flux, 7-26 October 2002.....	22

1. Introduction

The Upper Ocean Processes (UOP) group at the Woods Hole Oceanographic Institution (WHOI) has measured a suite of meteorological parameters from buoys and ships since it designed the first IMET (Improved Meteorology) systems (Hosom et al., 1995). The suite has included all the parameters required for making estimates of air-sea heat and momentum fluxes. Among these parameters is the downwelling longwave energy flux. Measurement of this flux is challenging. Its measurement to sufficient accuracy has encountered many problems and generated a considerable literature (Burns et al., 2003; Pascal and Josey, 2000; Ji and Tsay, 2000; Payne and Anderson, 1999; Fairall et al., 1998; Philipona et al., 1995; Dickey et al., 1994; Miskolczi and Guzzi, 1993; Alados-Arboledas, 1988; Albrecht et al., 1974). High accuracy measurements at sea have increased difficulties over land-based measurements. Recent climate research programs have required increased accuracy of air-sea heat flux estimates. The UOP group has striven to steadily improve its measurements, and the work described here is part of this attempt.

Until recently, the Eppley Precision Infrared Radiometer (PIR) was the only instrument available for measuring downwelling longwave irradiance. As manufactured by Eppley, the PIR is not well adapted for deployment at sea. Its aluminum radiation shield is fragile, the combination of stainless steel, aluminum, and bronze used in its construction do not stand up well in a salt atmosphere, and it is difficult to mount on a buoy. Payne and Anderson (1999) described the IMET PIR, their redesign of the Eppley PIR, and its calibration. It is made of machined aluminum, hard anodized and sealed, and coated with a tough, durable white paint. The IMET PIR is manufactured to UOP specifications by The Eppley Laboratory and has been successfully deployed on ships and buoys for approximately fifteen years.

During that time it has performed reliably but satellite transmissions on buoys and the general high level of electrical noise on ships has caused interference with the very small output voltages from the thermopile. To avoid the thermopile voltages, we have constructed and tested a prototype pyrgeometer, henceforth the LWT, in which all measurements are with thermistors; there is no thermopile. Since thermistors have been made with sufficient stabilities for at least a decade and the means exist to calibrate them to high accuracy, this seemed a sensible idea. We also present some results of what is probably the first long term comparison of two commercial longwave flux sensors: the Eppley PIR and the Kipp & Zonen CG4. The CG4 has been available since early 2000.

2. PIR Operation

As delivered, the Eppley PIR contains a battery circuit, which delivers a voltage approximately proportional to the incident longwave flux. Fairall et al. (1998) has shown that a more accurate estimate of the incident flux can be made by removing the battery circuit and recording the thermistor resistances and thermopile voltage directly as has been done in the work described herein.

The fundamental radiometer calibration equation for a pyrgeometer with a thermopile, and thermistors in the case and dome, (from equation 10 in Fairall et al., 1998) is:

$$H = \sigma T_s^4 + (T_s - T_c)[1 - (1 - \varepsilon_0)\rho]k / \varepsilon_0 + B\sigma(T_s^4 - T_d^4) \quad (1)$$

where H is the total longwave flux, σ is the Stefan-Boltzmann constant, T_s is the absolute temperature of the black surface of the thermopile cap (detector), T_c is the case temperature, ε_0 is the emissivity of the paint on the cap, ρ is the infrared reflection coefficient for the silicon dome, k is the thermal conductivity of the thermopile mount, B is a second calibration constant, and T_d is the absolute temperature of the dome. Also,

$$(T_s - T_c) = \alpha V \quad (2)$$

where, α is the thermopile sensitivity constant, 694 K-V⁻¹ for the PIR (J. Hickey 1993, personal communication), and V is the thermopile voltage in volts. Since the coefficient of $(T_s - T_c)$ is a constant, we can rewrite the equation as

$$H = \underset{1}{\sigma T_s^4} + \underset{2}{A(T_s - T_c)} + \underset{3}{B\sigma(T_s^4 - T_d^4)} \quad (3)$$

These three terms are in order of decreasing magnitude under most conditions. Term 2 in equation 3 can be loosely interpreted as the thermal conduction from the detector to the PIR body and term 3 as the radiation exchange between the detector and the dome. Each equation requires only three temperature measurements, T_s , T_c , and T_d . A can be expressed in terms of s_0 , the fundamental radiometer sensitivity constant by,

$$A = \frac{1}{s_0 \alpha} \quad (4)$$

For the Eppley PIR s_0 was computed from s_e , the Eppley calibration constant, by equation 19 from Fairall et al. (1998).

$$s_0 = \frac{s_e}{\{1 - 4\alpha s_e \sigma [1 + B(1 - f)] T_c^3\}} \quad (5)$$

where $f = 0.5$, $B = 3.5$, and $T_c = 22$ °C.

Kipp & Zonen give calibration constants for the Albrecht et al. (1974) radiometer equation:

$$H = \sigma T_c^4 + V / s \quad (6)$$

where

$$s^{-1} = [k / \tau + 4\varepsilon_0 T_c^3 (1 + \varepsilon / \tau)] \alpha \quad (7)$$

A photograph of the Kipp & Zonen CG4, the Eppley PIR and one of the thermistor pyrgeometers is shown in figure 1 and cross-sectional sketches of each in figures 2-4. Both the Kipp & Zonen and the Eppley have a thermistor to measure case temperature and a thermopile to measure the temperature difference between case and the blackened detector plate under the dome. The Eppley has a thermistor cemented to the inside of the dome to measure dome temperature. The Kipp & Zonen dome is quite flattened relative to a hemisphere and is thermally tightly coupled to the case. Kipp & Zonen believe that their dome configuration contributes a negligible amount to the radiation sensed by the detector plate. Thus, the last term in equation 1 is neglected for the CG4.

3. A New Pyrgeometer

Three fundamental changes were made from the Eppley PIR. All measurements are made with thermistors: There is no thermopile. The whole sensor is made of machined aluminum. One advantage is that the thermal conductivity is higher than either bronze or stainless steel, which should lead to smaller temperature gradients within the sensor. As a consequence of this and the white paint protecting the outer surface, we are able to dispense with the radiation shield. These shields are fragile and do not perform well on buoys. The blackened disk under the dome is 2.2 cm in diameter filling 63% of the area of the dome base. The equivalent surface in the Eppley PIR is 1.1 cm in diameter filling 17% of the area of the dome base.

The external shell of the LWT is machined aluminum, hard anodized and sealed, and coated with Ameron Siloxane PSX 700, a rugged, two-part, bright white paint containing both epoxy and acrylic polyurethane. The sides are at a 45-degree angle to the base to better reflect shortwave radiation. The silicon dome was purchased from the Eppley Laboratory.

The detector plate is supported by three 1.6 mm diameter stainless steel rods, which are cemented into the aluminum internal plug. The plug is also hard anodized and attached to the shell by four screws. Two versions were assembled. The detector plate in one was a disk of 1.3 mm thick machined of aluminum; in the other it was a 0.1 mm thick aluminum disk cut from a soft drink can. Both disks were coated on their upper surfaces with Parson's Black optical lacquer purchased from the Eppley Laboratory.

The LWT was designed to accommodate up to seven thermistors. Of the three thermistors potted in the base plug, one was 2.5 mm below its top surface under the middle of the detector plate, one was 2.5 mm below the bottom of the detector support rods, and one was at a location in the plug away from other holes. One thermistor was cemented to the underside of the detector plate with conducting epoxy. Up to three thermistors can be cemented to the inside of the dome. LWT001 had three thermistors approximately 120 degrees apart and about 30 degrees above the dome base. LWT002 had a single thermistor about 30 degrees above the dome base. For test purposes, multiple thermistors were installed to monitor temperature gradients within the pyrgeometers.

Two types of thermistors were used, both glass-encapsulated for high stability. Thermometrics type BR55KB303K has a diameter of only 1.3 mm and was used for minimum physical size and

thermal mass. Our extensive experience with Thermometrics epoxy-encapsulated thermistors is that they drift less than 2 mK/year. Glass encapsulation is well known to improve stability of thermistors. YSI type 46032 has a diameter of 2.2 mm and YSI states that the typical thermometric drift of this type is less than 10 mK in 100 months. The Thermometrics was used in the dome of both sensors and under the detector plate of LWT002. The YSI thermistor was used everywhere else. Both types have a nominal resistance of 30 k Ω at 20°C.

In parallel with the pyrgeometer development, we built two IMET modules designed to record data from up to seven thermistors. Each thermistor has a 0.1% Vishay resistor in series. Five volts are applied to all seven resistor/thermistor pairs resulting in a current of 30-90 microamp depending on the thermistor temperature. The channels are individually calibrated using a set of Vishay 0.01% resistors, equivalent to about 2 mK for both thermistor types used in the LWTs. Once per minute, sixteen scans of the seven thermistor voltages and the 5 volt exciting voltages are made in 1.05 s, and the averages of the 16 samples are recorded on a PCMCIA card with time and date. Resolution of an individual sample is equivalent to 4 mK/count. Power dissipated in the thermistors is less than 200 μ W. YSI gives a dissipation constant of 10 mW/°C in stirred oil. Assuming that the potted thermistors have at least as good heat sinking as stirred oil, the short time that the current is applied will result in self-heating of less than 0.02 K. Similar self heating occurs during the thermistor calibration. Altogether, then, we expect an accuracy of about 0.01 K in our temperature measurements.

4. Accuracy

In order to make an estimate of the measurement accuracy, it will be assumed that the errors are all independent. The uncertainty can be written as:

$$(\delta H)^2 = \left(\frac{\partial H}{\partial A} \delta A\right)^2 + \left(\frac{\partial H}{\partial T_s} \delta T_s\right)^2 + \left(\frac{\partial H}{\partial T_c} \delta T_c\right)^2 + \left(\frac{\partial H}{\partial T_d} \delta T_d\right)^2 + \left(\frac{\partial H}{\partial B} \delta B\right)^2 \quad (8)$$

Or

$$(\delta H)^2 = ((T_s - T_c)\delta A)^2 + \left\{4\sigma(1+B)T_s^3 + A\right\}^2 \delta T_s^2 + (A\delta T_c)^2 + (4B\sigma T_d^3 \delta T_d)^2 + (\sigma(T_s^4 - T_d^4)\delta B)^2 \quad (9)$$

From our thermistor calibrations, the uncertainty in T_s and T_c is 0.01 K. That in T_d is probably larger from self-heating since the dome is a poorer heat sink and from gradients (Philipona et al., 1995) so we estimate that as 0.1 K. The variation in A and B through a number of repeat calibrations of Eppley PIRs is about 5%. For LWT001, $(T_s - T_c)$ is about 0.4 K, T_s and T_d vary between 275 K in winter to 300 K in summer, A is 200, B is 3.7, and $\sigma(T_s^4 - T_d^4)$ is of order 2. H varies from 300 to 400 W m⁻². Combining these we get,

$$(\delta H)^2 = 16.0 + 0.07 + 4.0 + 0.04 + 0.14 = 20.3 \quad (10)$$

or an uncertainty in H of 4.5 W m^{-2} , about 1.5 % which agrees with the estimate by Fairall et al., (1998) for the Eppley PIR. The dominant term in this calculation is from the uncertainty in A.

5. Calibration

The thermistors were calibrated in a water bath to an accuracy of $\pm 0.005 \text{ K}$ using a National Institute of Science and Technology traceable model SBE35 thermometer made by Sea-Bird Electronics. The data were fitted to the Steinhart-Hart (Steinhart and Hart, 1968) equation:

$$\frac{1}{T} = a + b \log(R) + c(\log(R))^3 \quad (11)$$

where R is the thermistor resistance in ohms, the log is to base e, and a,b,c are the calibration constants. T is computed in kelvins.

We had anticipated calibrating the thermistor pyrgeometers by the method of Payne and Anderson (1999) in which the A constant is computed at times when the detector plate temperature is equal to that of the dome and LW3 in equation 3 is zero. However, the slower response times of the new sensor's detector plate meant that LW2 and LW3 passed through zero at approximately the same time. Instead, we arbitrarily assumed that the Kipp & Zonen values were the most reliable and did a least squares fit of equation 3 to the Kipp & Zonen CG4 total longwave fluxes for the entire data set, determining values of A and B for LWT001 and LWT002. Table 1 shows the calibration constants for the two thermistor pyrgeometers and the Eppley PIR. LWT001 contains the 1.3 mm disk, LWT002 the 0.1 mm disk. The differences in the A constant are striking.

Table 1: Calibration Constants

Sensor	A	B
Eppley 26982	366.0	3.0
LWT001	200.4	3.7
LWT002	101.2	4.4

6. Data Set

UOP maintains a radiometer calibration facility on the roof of the Clark Laboratory on the Quissett Campus of the Woods Hole Oceanographic Institution. This facility, shown in figure 5, has a totally unobstructed view of the sky. It is designed to allow careful leveling of up to 8 IMET radiometer modules, as well as mounting up to 5 standard radiometers to be recorded on a Campbell Scientific CR7 data logger. During all of 2002, a set of three longwave radiometers and a single shortwave radiometer were mounted on this facility. Thermistors were measured by applying a precision voltage to the thermistor and a Vishay fixed resistor in series with it and by digitizing the voltage across the thermistor. These voltages and the thermopile voltage were sampled once per 3 s. One-minute averages were recorded by the CR7. The longwave sensors included a recently purchased Kipp & Zonen CG4, an Eppley PIR, and an IMET PIR (Payne and

Anderson, 1999). The shortwave radiometer was an Eppley PSP manufactured by Eppley for the UOP group to a design similar to that of the IMET PIR, i.e., white-painted machined aluminum with no shield. The equation and calibration constants supplied by Kipp & Zonen were used for the CG4. Their equation is, effectively, equation 3 with no LW3 term, and with T_c substituted for T_s in LW1. The Eppley Laboratory calibration constant of the PIR was used to compute its A constant as described in section 3 although the PIR thermistors were calibrated in our laboratory to the same accuracy as the LWT thermistors.

The claim by Kipp & Zonen that their dome design obviates the necessity of measuring dome temperature seems to be valid: A careful perusal of the entire data set showed no cases of elevated CG4 readings over the PIR caused by solar radiation.

Both thermistor pyrgeometer modules were deployed on the roof for nearly a year, from January 27 through December 31, 2002, except for two gaps: 18 April to 30 May and 7-29 August. The thermistor resistances were converted to temperatures and then to longwave fluxes. These module files and the processed CR7 file were averaged to a 10-minute series for analysis.

7. Anomalous Data

There were 40 occasions during the year when both the thermistor pyrgeometers recorded total longwave flux values that were 20 W m^{-2} or more higher than the Kipp & Zonen for periods of 2-14 hours. Most of these periods began during the night and ended sometime after sunrise. During 11 of these periods the IMET PIR also showed similarly elevated values, although of lesser amplitude. Since most of the anomalous data occurs at night, we ruled out shortwave leakage of the domes as a possible cause. Figure 6 shows one example of anomalous LWT values. In Figure 7 both the LWTs and the Eppley PIR are anomalous compared to the Kipp & Zonen CG4. There was no rain during any of the days in the figures. The anomalies in each case occur in LW2, the thermopile voltage term. When these anomalies occur, there is no identifiable common feature linking those instruments, which deviate from the rest. The anomalous data represent 6.9% of the total and are fairly evenly distributed through the year.

We have not seen another long-term comparison between the CG4 and the PIR. It is disturbing that during the 9.2 month data series there were a total of 11 events when the PIR values were anomalously high by 20 W m^{-2} or more compared to the CG4. In each case, the anomaly appeared to be in LW2, the term containing the thermopile voltage.

8. Comparison

Since the Kipp & Zonen does not have a term analogous to term 3 in equation 3, and since it was used to calibrate the LWTs, we compared the LWTs with the Eppley PIR. Figures 8 and 9 are plots of LWT001 and LWT002 total longwave flux vs. the Eppley PIR. The line in each plot represents a least squares linear fit of the data. The agreement is within approximately 5 W m^{-2} over the whole range. LWT002 has somewhat less scatter than LWT001. This may be from the thinner detector plate and smaller thermistor in LWT002 yielding a slightly shorter time constant. Table 2 gives the mean and standard deviation of the differences between the two LWTs, the Eppley and the Kipp & Zonen for the anomaly-free data series and for the full data

series containing the anomalies. Although the mean differences are only slightly different, the standard deviations are nearly doubled when the anomalies are included.

Table 2: Pyrgeometer mean differences and standard deviations, 9.2 months of data
Units are $W m^{-2}$

<u>Difference</u>	No Anomalies		All data	
	<u>LWdiff</u>	<u>SD</u>	<u>LWdiff</u>	<u>SD</u>
LWT001-K&Z	-0.5	4.4	1.1	8.5
LWT001-Eppley	0.8	5.3	1.2	8.2
LWT002-K&Z	0.9	2.7	2.3	7.3
LWT002-Eppley	2.1	3.1	2.4	6.7
Eppley-K&Z	-1.3	2.5	-0.1	3.5

It is encouraging that the anomalies do not affect the long-term averages appreciably and that the long term means agree within $1-2 W m^{-2}$. The combination of these mean results and the anomalies mentioned previously indicates to us, however, that, although long-term averages can be accurate, there is a possibility of errors amounting to tens of $W m^{-2}$ in measurements on time scales of hours.

We also carried out a comparison over a 20-day period, which contained no anomalies, from 7 to 26 October. Figure 10 shows the total longwave flux for all four sensors, the CG4, the PIR, and the two LWTs. Figure 11 shows the difference between the Kipp & Zonen and the two LWTs. Figure 12 shows the same for the Kipp & Zonen and the Eppley. Figure 13 shows the shortwave flux for the period. Table 3 shows the mean differences and standard deviations for these data. Differences and standard deviations are of the same order as for the whole data set.

Table 3: Pyrgeometer mean differences and standard deviations, year day 280-299
Units are $W m^{-2}$

Difference	LWdiff	SD
LWT001-K&Z	-0.6	4.2
LWT001-Eppley	0.3	4.4
LWT002-K&Z	1.1	2.3
LWT002-Eppley	2.0	1.5
Eppley-K&Z	-0.9	1.7

Lastly, to show the degree of agreement between the four pyrgeometers and the effects of ignoring the anomalies, Table 4 contains flux values averaged over the whole 9.2 months, with and without the periods containing anomalous data. The agreement is excellent and the anomalies cause an elevation of the PIR and LWT averages by only about $1 W m^{-2}$ relative to the CG4.

Table 4: Overall longwave flux averages
Units are W m^{-2}

Sensor	No Anomalies	All Data
Kipp & Zonen CG4	313.6	312.8
Eppley PIR	312.3	312.7
LWT001	313.1	314.0
LWT002	314.5	315.1

9. Conclusion

A pyrgeometer, intended particularly for deployment on ships and buoys, has been designed, and two have been built and tested in a comparison with a Kipp & Zonen CG4 and an Eppley PIR. The comparison data set consists of a total of 9.2 months of 1-minute averages recorded between January and December 2002 in Woods Hole, Massachusetts.

When averaged over the whole data set, all four pyrgeometers are consistent to 2.2 W m^{-2} or better. Standard deviations of the differences of the two LWTs relative to the Kipp & Zonen are, however, at least twice that of the Eppley. The standard deviations of all three represent significant differences on time scales of hours. The LWTs have many more periods of such anomalies than does the Eppley. Since nearly all of the anomalous periods begin before dawn, shortwave radiation cannot be involved. Several of the periods occurred during a very dry, rainless period so moisture on the outside of the domes is unlikely to be a factor. We intend to continue our observations by recording additional environmental parameters such as relative humidity, precipitation, and wind speed to try to find the cause of the anomalies.

We conclude that contemporary thermistors allow temperature measurements of sufficient accuracy that the thermopile can be eliminated from pyrgeometers although our design is not optimum. We also conclude that differences seen between the Kipp & Zonen CG4 and the Eppley PIR raise doubts about their absolute accuracies on time scales of hours although their long-term averages are quite comparable.

10. Acknowledgments

Steven Anderson helped initiate this study and contributed many constructive suggestions in the initial phases. Discussions of the analysis with Frank Bradley were most helpful as were his comments on the manuscript. Construction of the LWTs was ably carried out by Mark St. Pierre of the WHOI machine shops. Design and programming of the LWT IMET modules was by Geoffrey Allsup. Funding was through National Science Foundation Grant OCE98-18470.

11. References

- Alados-Arboledas, L., J. Vida, and J. I. Jimenez, 1988. Effects of solar radiation on the performance of pyrgeometers with silicon domes. *Journal of Atmospheric and Oceanic Technology*, **5**, 666-670.
- Albrecht, B. A., M. Poellot and S. K. Cox, 1974. Pyrgeometer measurements from aircraft. *Rev. Sci. Instrum.*, **15**, 33-38.
- Burns, J. Sun, A. C. Delaney, S. R. Remmer, S. P. Oncley, and T. W. Horst, 2003. A field intercomparison technique to improve the relative accuracy of longwave radiation measurements and an evaluation of CASES-99 pyrgeometer data quality. . *Journal of Atmospheric and Oceanic Technology*, **20**, 348-361.
- Dickey, T. D., D.V. Manov, R. A. Weller, and D. A. Siegel, 1994. Determination of longwave Heat Flux at the air-sea interface using measurements from buoy platforms. *Journal of Atmospheric and Oceanic Technology*, **11**, 1057-1078.
- Fairall, C. W., P. O. G. Persson, E. F. Bradley, R. E. Payne and S. P. Anderson, 1998. A new look at calibration and use of Eppley Precision Infrared Radiometers. Part I.: Theory and application. *Journal of Atmospheric and Oceanic Technology*, **15**, 1229-1242.
- Hosom, D. S., R. A. Weller, R. E. Payne and K. R. Prada, 1995. The IMET (Improved Meteorology) Ship and buoy system. *Journal of Atmospheric and Oceanic Technology*, **12**, 527-540.
- Ji, Qiang and Si-Chee Tsay, 2000. On the dome effect of Eppley pyrgeometers and pyranometers. *Geophysical Research Letter*, **27**, 971-974.
- Miskolczi, F. and R. Guzzi, 1993. Effect of nonuniform spectral dome transmittance on the accuracy of infrared radiation measurements using shielded pyrrometers and pyrgeometers. *Applied Optics*, **32**, 3257-3265.
- Pascal, R. W., and S. A. Josey, 2000. Accurate radiometric measurement of the atmospheric longwave flux at the sea surface. *Journal of Atmospheric and Oceanic Technology*, **17**, 1271-1282.
- Payne, R. E. and S. P. Anderson, 1999. A new look at calibration and use of Eppley Precision Infrared Radiometers. Part II: Calibration and use of the Woods Hole Oceanographic Institution Improved Meteorology Precision Infrared Radiometer. *Journal of Atmospheric and Oceanic Technology*, **16**, 739-751.

Philipona, R., C. Frohlich, and Ch. Betz, 1995. Characterization of pyrgeometers and the accuracy of atmospheric longwave radiation measurements. *Applied Optics*, **34**, 1598-1605.

Steinhart, J. S. and S. R. Hart, 1968. Calibration curves for thermistors. *Deep-Sea Research*, **15**, 497-503.



Figure 1: L/R: The Eppley PIR, Kipp & Zonen CG4, and a thermistor pyrometer.

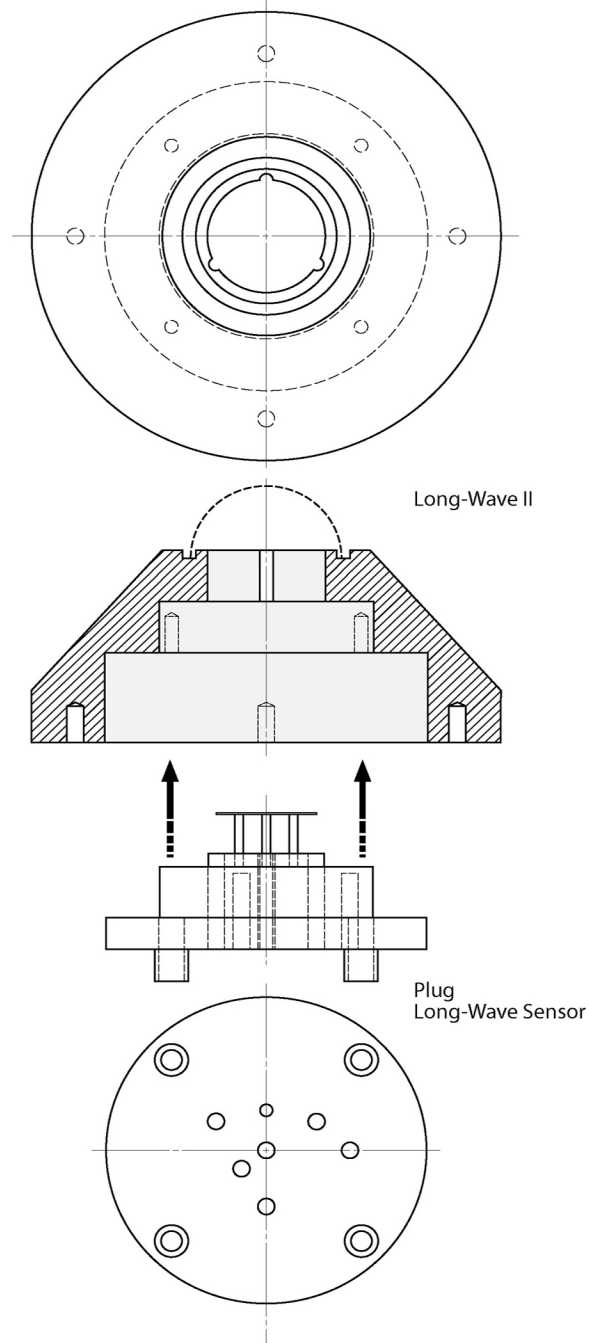


Figure 2: Cross-section sketch of the all-thermistor pyrgeometer.

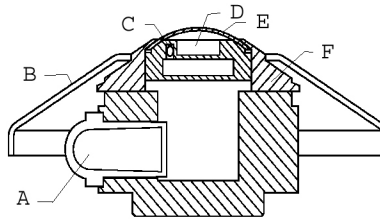


Figure 3: Sketch of the Kipp & Zonen CG4 pyrgometer. Labeled parts are: (A) desiccant; (B) white sun screen; (C) body temperature thermistor; (D) thermal detector; (E) silicon window; (F) sub frame.

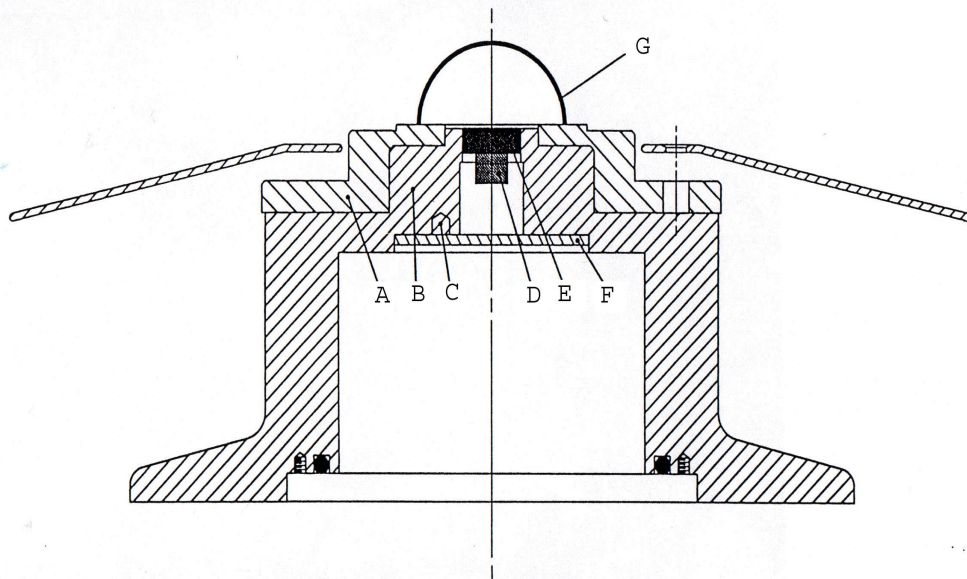


Figure 4: Sketch of the Eppley PIR. (A) top and dome mount (stainless steel); (B) pyrgometer body (cast bronze); (C) hole in which body thermistor is potted; (D) thermopile; (E) thermal detector; (F) internal radiation shield (aluminum); and (G) silicon window.



Figure 5: Radiometer calibration facility on roof of Clark Laboratory, Woods Hole, MA. The Kipp & Zonen CG4, Epply PIR, Epply/IMET PSP and Epply/IMET PIR are in the foreground. An LWT is at the top of each of the two long tubes just beyond.

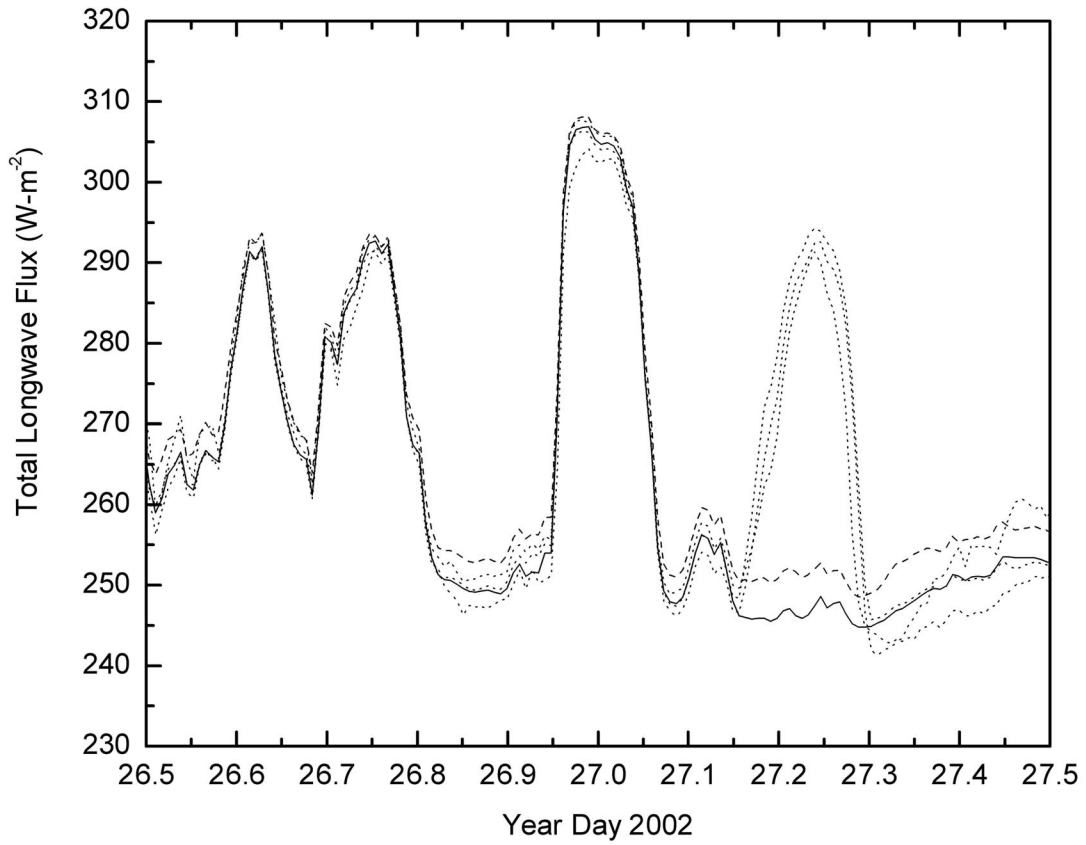


Figure 6: Example of elevated values of total longwave flux of LWT001, LWT002 and IMET PIR (dotted lines) relative to the Kipp & Zonen CG4 (solid line) and Eppley PIR (dashed line).

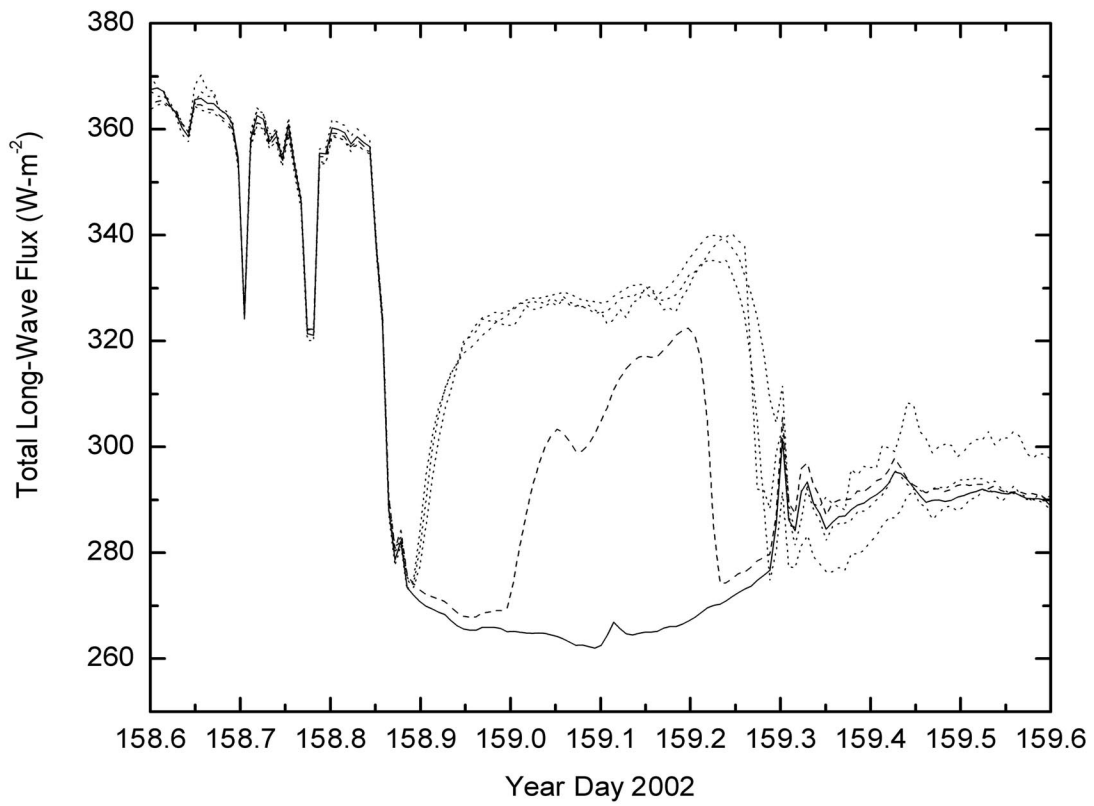


Figure 7: Example of elevated values of total longwave flux of the LWT001, LWT002 and the IMET PIR (dotted lines) and the Eppley PIR (dashed line) relative to the Kipp & Zonen CG4 (solid line).

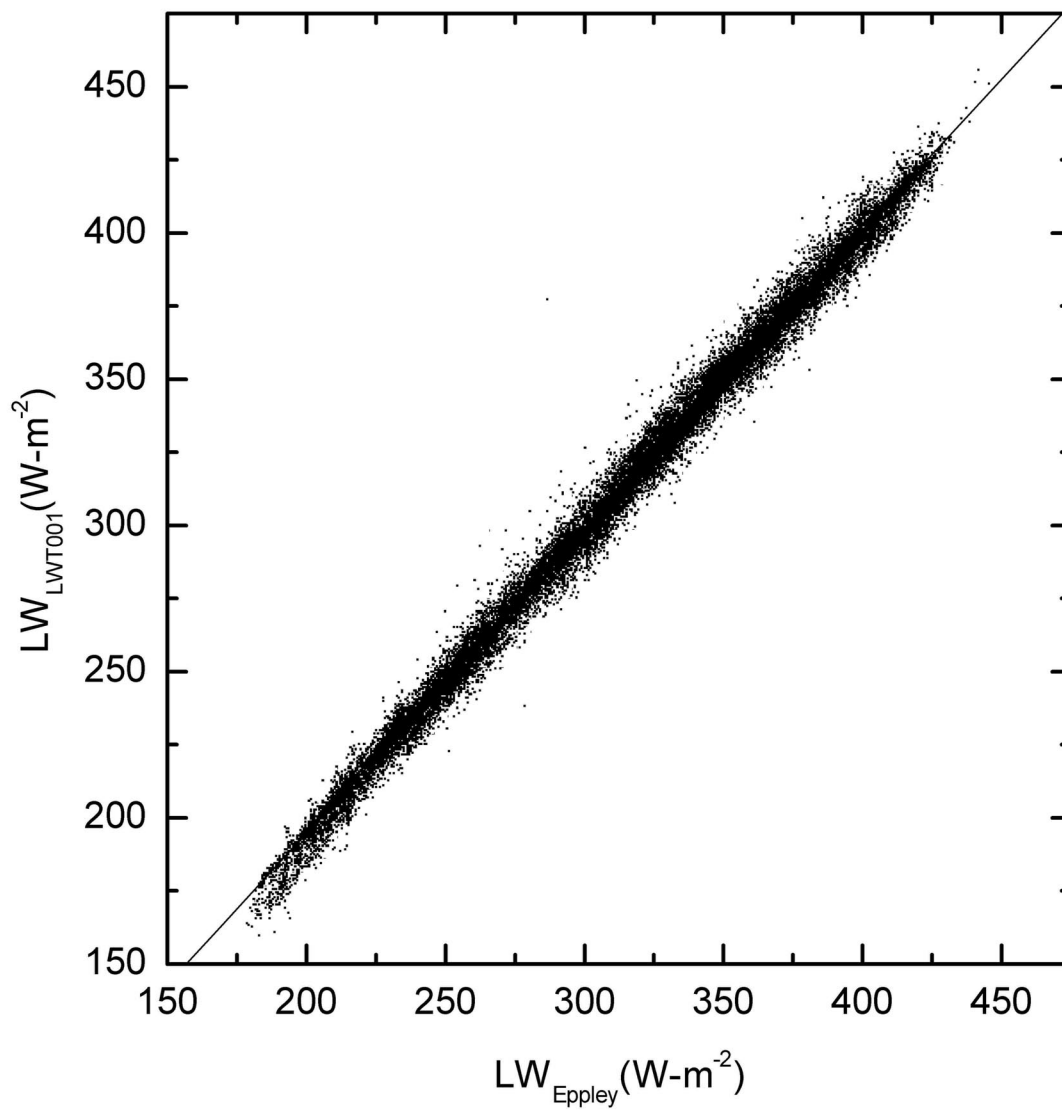


Figure 8: Total longwave flux of thermistor pyrometer LWT001 vs. Eppley PIR.

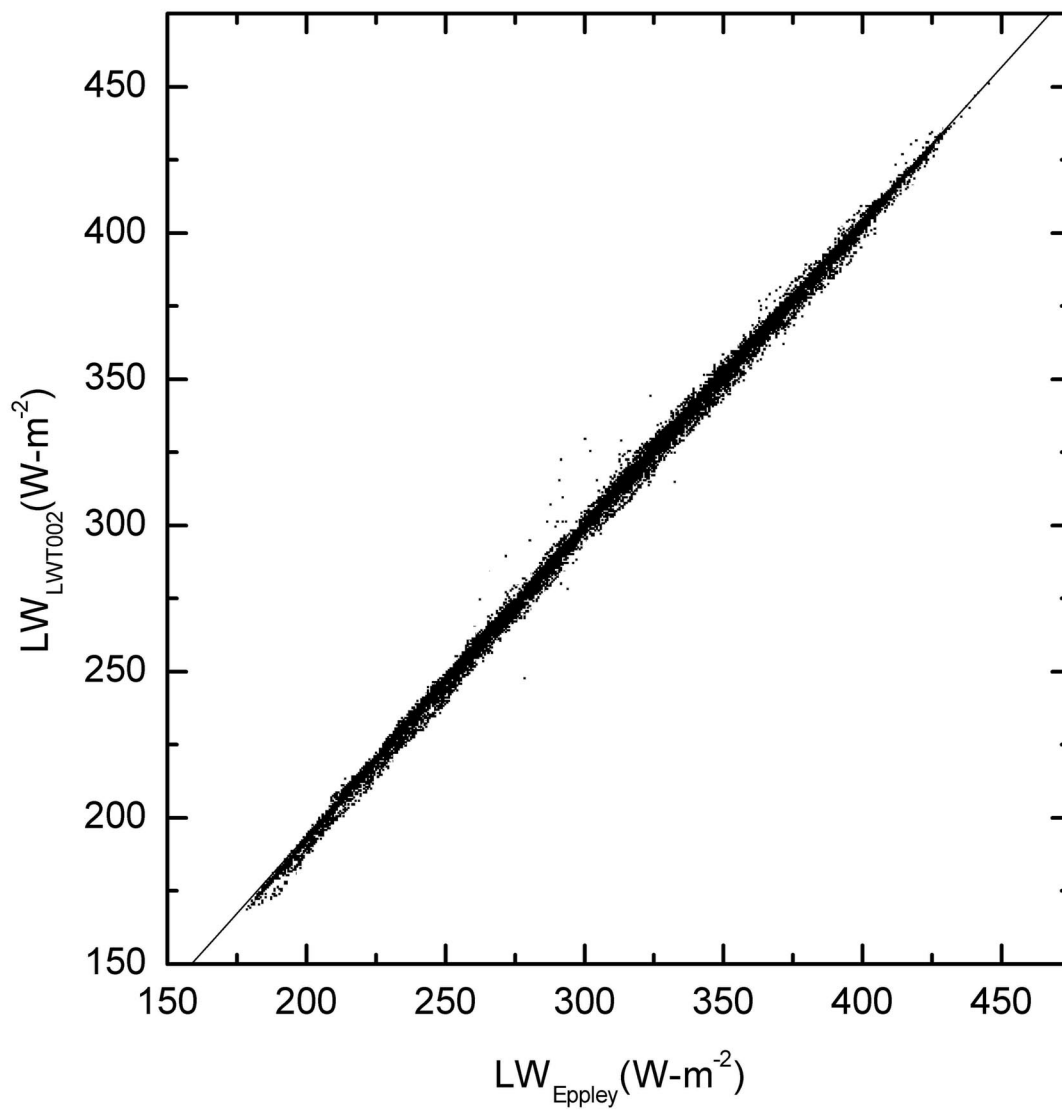


Figure 9: Total longwave flux of thermistor pyrgometer LWT002 vs. Eppley PIR.

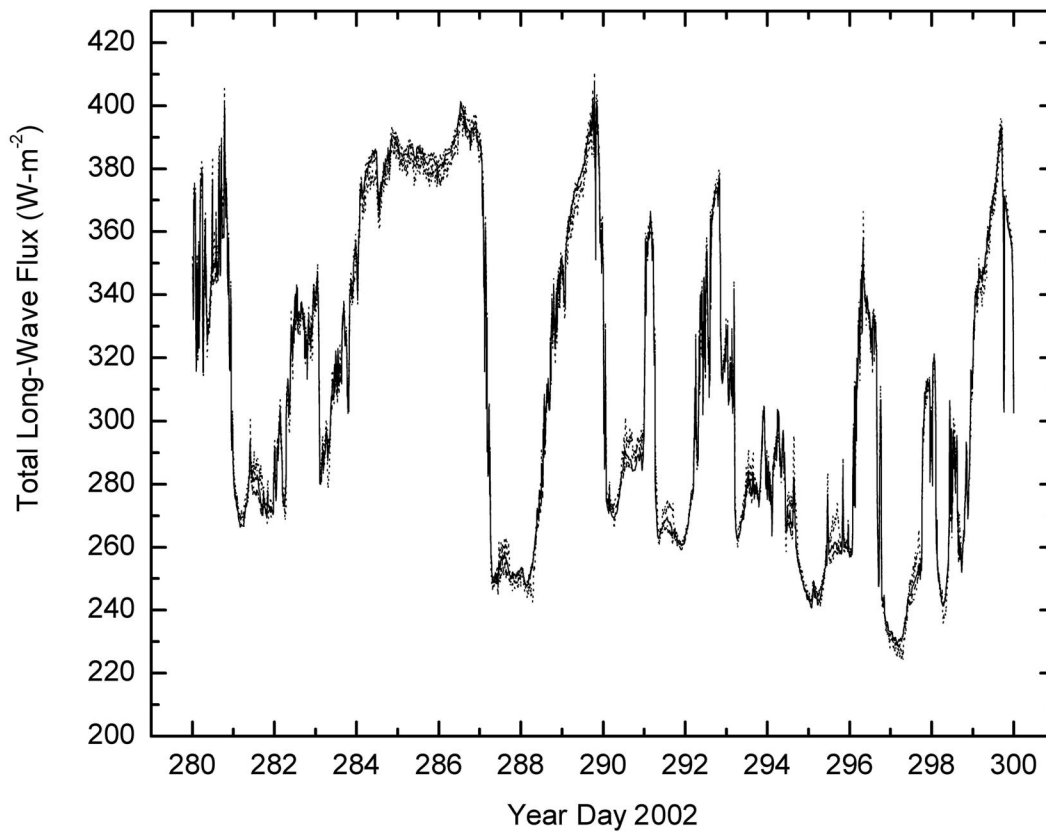


Figure 10: Total longwave flux of Kipp & Zonen CG4 (solid line), Eppley PIR (dashed line), and LWT001, LWT002 (dotted lines), 7-26 October 2002.

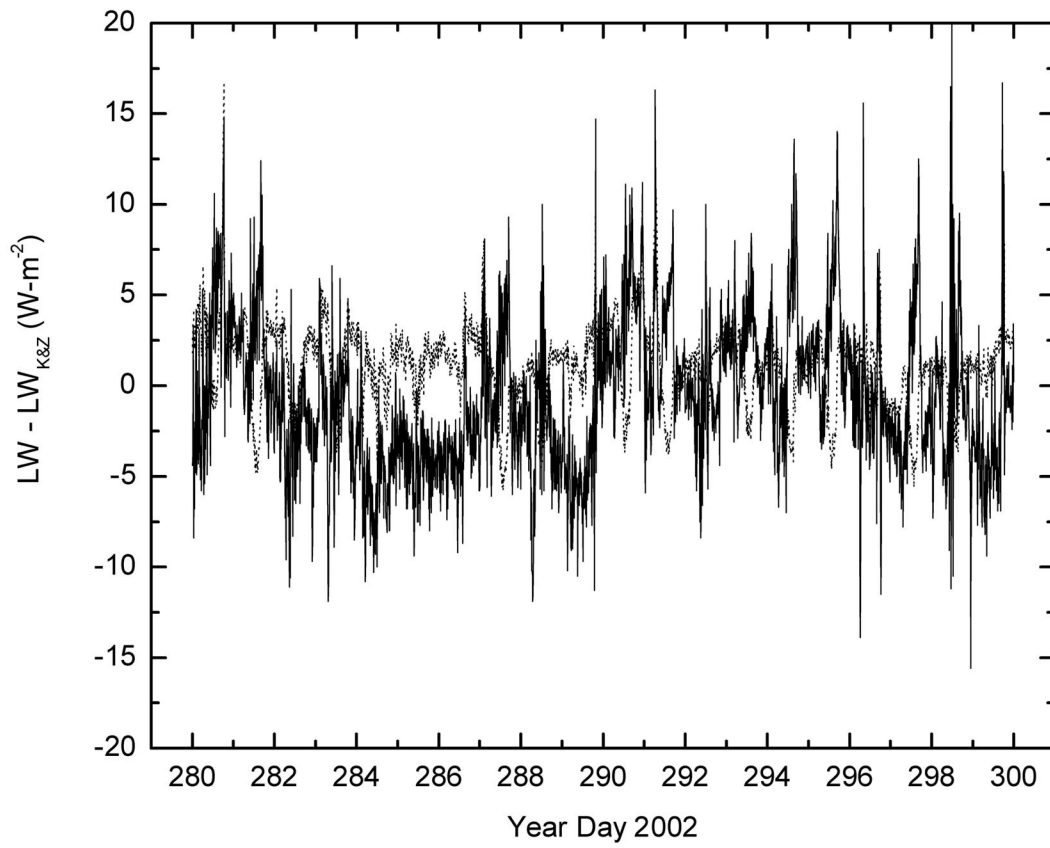


Figure 11: Difference between LWT001 (solid line), LWT002 (dotted line) and Kipp & Zonen CG4 total longwave fluxes, 7-26 October 2002.

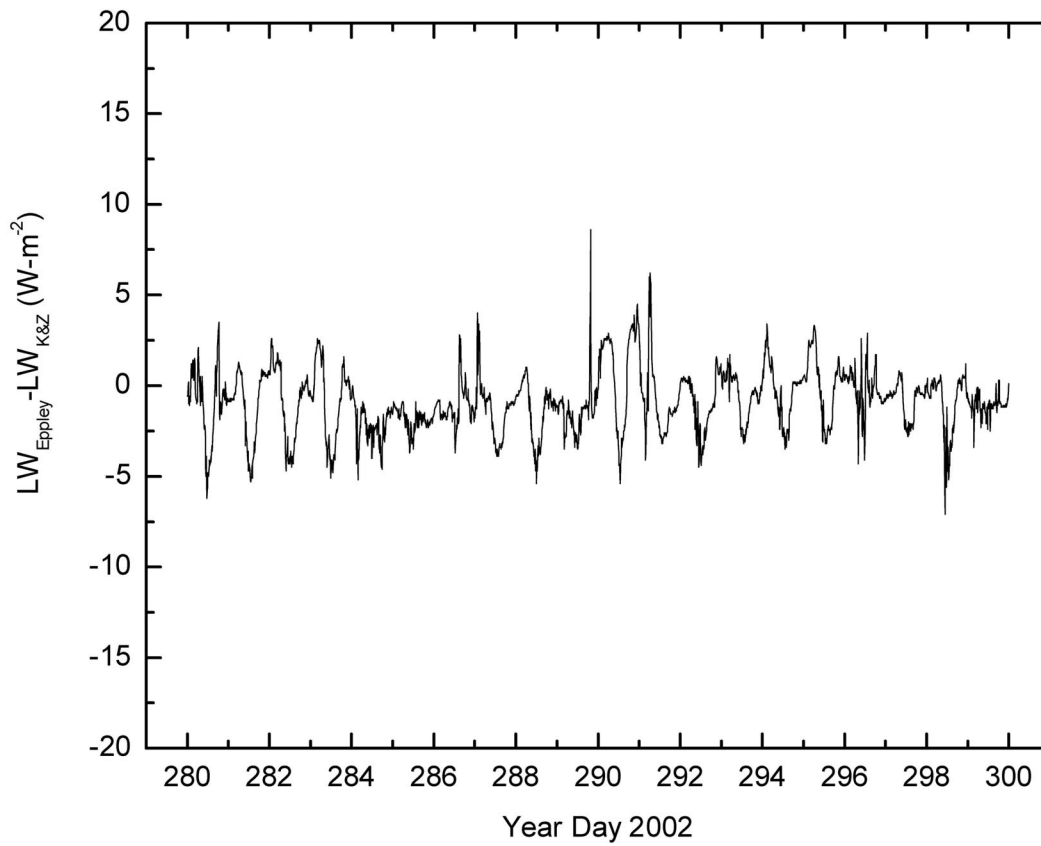


Figure 12: Difference between Eppley PIR and Kipp & Zonen CG4 total longwave fluxes, 7-26 October 2002.

DOCUMENT LIBRARY

Distribution List for Technical Report Exchange – July 1998

University of California, San Diego
SIO Library 0175C
9500 Gilman Drive
La Jolla, CA 92093-0175

Hancock Library of Biology & Oceanography
Alan Hancock Laboratory
University of Southern California
University Park
Los Angeles, CA 90089-0371

Gifts & Exchanges
Library
Bedford Institute of Oceanography
P.O. Box 1006
Dartmouth, NS, B2Y 4A2, CANADA

NOAA/EDIS Miami Library Center
4301 Rickenbacker Causeway
Miami, FL 33149

Research Library
U.S. Army Corps of Engineers
Waterways Experiment Station
3909 Halls Ferry Road
Vicksburg, MS 39180-6199

Marine Resources Information Center
Building E38-320
MIT
Cambridge, MA 02139

Library
Lamont-Doherty Geological Observatory
Columbia University
Palisades, NY 10964

Library
Serials Department
Oregon State University
Corvallis, OR 97331

Pell Marine Science Library
University of Rhode Island
Narragansett Bay Campus
Narragansett, RI 02882

Working Collection
Texas A&M University
Dept. of Oceanography
College Station, TX 77843

Fisheries-Oceanography Library
151 Oceanography Teaching Bldg.
University of Washington
Seattle, WA 98195

Library
R.S.M.A.S.
University of Miami
4600 Rickenbacker Causeway
Miami, FL 33149

Maury Oceanographic Library
Naval Oceanographic Office
Building 1003 South
1002 Balch Blvd.
Stennis Space Center, MS, 39522-5001

Library
Institute of Ocean Sciences
P.O. Box 6000
Sidney, B.C. V8L 4B2
CANADA

National Oceanographic Library
Southampton Oceanography Centre
European Way
Southampton SO14 3ZH
UK

The Librarian
CSIRO Marine Laboratories
G.P.O. Box 1538
Hobart, Tasmania
AUSTRALIA 7001

Library
Proudman Oceanographic Laboratory
Bidston Observatory
Birkenhead
Merseyside L43 7 RA
UNITED KINGDOM

IFREMER
Bibliothèque La Pérouse
Centre de Documentation sur la Mer
15 rue Dumont d'Urville
Technopôle Brest-Iroise
BP 70 — 29280 Plouzané — FRANCE